Fast-convergent Fault Detection and Isolation in an Uncertain Scenario

Peng Li, Francesca Boem, Gilberto Pin, Thomas Parisini

***Abstract*— In this paper, a fast-convergent fault detection and isolation architecture is proposed for linear MIMO continuous-time systems. By exploiting a system decomposition technique and making use of kernel-based deadbeat estimators, the state variables can be estimated in a non-asymptotic way. Estimation residuals are then defined to detect the occurrence of a fault and identify the occurring fault function after fault detection. In the noisy scenario, thresholds are defined for the residual to distinguish the effect of the noise from that of the fault. Numerical examples are included to characterize the effectiveness of the proposed FDI architecture.**

I. Introduction

Fault Detection and Isolation (FDI) is a fundamental research field for modern engineering systems. Reliable FDI schemes are needed, able to accurately monitor the status of the system and rapidly diagnose the fault before it has the chance to destabilize the system or lead to more severe system failures. For preliminaries and typical FDI techniques, readers can refer to the books [1], [2], [3].

Model-based FDI methodologies are a powerful class of tools to address the fault diagnosis problem, relying on state observation, parameter estimation, identification and/or parity equations techniques [4]. The main logic consists in the analysis of Input/Output signals, compared to the expected nominal behavior based on the model of the system. Remarkably, thanks to the development of the communication technologies, distributed FDI methods have been developed suitable for large-scale systems, *e.g.* [5], [6], [7], [8], [9]. Typical estimation methods for FDI guarantee asymptotic convergence, which means the estimation error will decrease gradually to the neighborhood of zero. Moreover, the choice of initial conditions may affect the estimates. As a consequence, slow convergence of the estimators (and possibly of the thresholds as consequence) may cause inaccuracy, delays in the detection of faults and misdetection or false-alarms. Furthermore, in many FDI schemes, separate estimators are needed to achieve fault detection and isolation respectively. Therefore, after the detection of the fault, a further transient is needed before the fault can be isolated, thus increasing the duration of the whole fault diagnosis process. Therefore, estimation methods with fast convergence are desired.

This work has been supported by European Union's Horizon 2020 research and innovation programme under grant agreement No 739551 (KIOS CoE).

P. Li is with the Dept. of Electronic and Electrical Engineering, Imperial College London (UK) (peng.li13@imperial.ac.uk); F. Boem is with the Dept. of Electronic and Electrical Engineering, University College London, UK. (f.boem@ucl.ac.uk; G. Pin is with Electrolux Professional S.p.A., Italy (gilberto.pin@electrolux.it); T. Parisini is with the Dept. of Electrical and Electronic Engineering at the Imperial College London, UK, with the KIOS Research and Innovation Centre of Excellence, and also with the Dept. of Engineering and Architecture at University of Trieste, Italy. (t.parisini@gmail.com).

In the context of fast-converging estimation, a kernel-based deadbeat estimation methodology is proposed in [10]. Making use of the Volterra integral operator induced by suitably designed kernel functions, the kernel-based methodology removes the effect of the unknown initial conditions thus achieving non-asymptotic convergence without transient phase. Paradigms have been proposed for parameter estimation [10], state estimation [11] and state-parameter joint estimation [12]. Remarkably, the state-parameter joint estimation has been successfully utilized for FDI of interconnected systems in [13], where the possible fault functions are assumed to depend on the measurements.

In this work, a novel robust FDI scheme with fast convergence is proposed, able to detect and isolate faults which may depend on non-directly measured state variables. Indeed, applying the deadbeat observer to a system decomposed as suggested in [14] (to be discussed thereafter), allows to reconstruct the fault signals even if they are functions of the internal state variables. Moreover, the Volterra image of the fault signal can be estimated and compared with the counterparts of the reconstructed possible fault functions, to achieve fast fault isolation. The robustness of the proposed FDI scheme in presence of both measurement and process noises is analyzed and a modified FDI scheme is proposed for this scenario, by defining suitable detection and isolation thresholds, guaranteeing the absence of false-alarms. Numerical examples are included to verify the effectiveness of the proposed FDI method.

II. Problem statement

Consider a system modeled as:

$$\mathcal{S}: \begin{cases} \dot{x}(t) &= Ax(t) + Bu(t) + Ef(t,x,u) \\ y(t) &= Cx(t) \end{cases} \tag{1}$$

where $x(t) \in \mathbb{R}^n$, $u(t) \in \mathbb{R}^m$ and $y(t) \in \mathbb{R}^q$ are the state, the input and the output variables of the system respectively. The continuous function $f(t,x,u) \in \mathbb{R}^p$ models the effects of a general fault on the state dynamic equation. A, B, C, E are constant matrices with appropriate dimensions. The fault function is modeled as

$$f(t,x,u) = \mathcal{B}(t-T_0)\phi(t,x,u),$$

where $\mathcal{B}(t-T_0)$ defines the fault time profile, which is equal to 0 before the unknown fault time T_0 and 1 after. $\phi(t,x,u) \in \mathbb{R}^p$ represents the functional structure of the fault. We exploit the transformation in [14] decomposing the system into two coupled subsystems, where the fault directly affects only the state of the first subsystem. The following assumptions are required as in [14]:

Assumption 1: $rank(CE) = rank(E)$.
This assumption indicates that the number of the outputs is greater than the dimension of the effective unknown fault.

Assumption 2: For every complex number λ with nonnegative real part

$$rank \begin{bmatrix} A - \lambda I & E \\ C & 0 \end{bmatrix} = n + rank(E).$$

Based on Lemma 1 in [14], Assumption 1 is equivalent to the existence of state and output transformations

$$x(t) = T \left[\zeta_1^\top(t)\ \zeta_2^\top(t)\right]^\top, \quad y(t) = S \left[\eta_1^\top(t)\ \eta_2^\top(t)\right]^\top$$

resulting in the decomposition of system (1) into the decomposition of system (1) into two transformed linear systems with the following structure

$$\mathcal{S}_{\zeta_1}: \begin{cases} \dot{\zeta}_1(t) = A_{11}\zeta_1(t) + A_{12}\zeta_2(t) + B_1 u(t) + E_1 f(t,x,u) \\ \eta_1(t) = C_{11}\zeta_1(t) \end{cases}$$

$$\mathcal{S}_{\zeta_2}: \begin{cases} \dot{\zeta}_2(t) = A_{21}\zeta_1(t) + A_{22}\zeta_2(t) + B_2 u(t) \\ \eta_2(t) = C_{22}\zeta_2(t) \end{cases} \tag{2}$$

with

$$T^{-1}AT = \begin{bmatrix} A_{11} & A_{12} \\ A_{21} & A_{22} \end{bmatrix} \quad S^{-1}CT = \begin{bmatrix} C_{11} & 0 \\ 0 & C_{22} \end{bmatrix}$$
$$T^{-1}B = \begin{bmatrix} B_1^\top & B_2^\top \end{bmatrix} \qquad T^{-1}E = \begin{bmatrix} E_1^\top & 0 \end{bmatrix},$$

where B_1 and C_{11} have the same number of rows with B_1 full row rank and C_{11} invertible. Thanks to Assumption 2, the pair (A_{22}, C_{22}) is detectable. Meanwhile, $\zeta_1(t) \in \mathbb{R}^{p_\star}$, $p_\star \triangleq rank(CE)$ and $\zeta_2(t) \in \mathbb{R}^{(n-p_\star)}$. Detailed calculation of the transformations and properties can be found in [14].

III. Non-asymptotic observer and fault diagnoser design

In this section we design a deadbeat estimator based on the decomposed system (2). The estimator exploits the Volterra operator algebra [15] and the adoption of non-asymptotic kernel functions [10], [11]. Remarkably, the estimator is able to non-asymptotically estimate both the state variables insensitive to the occurrence of the fault and the image of the unknown fault functions which are significant clues in the fault diagnosis.

A. State estimation

For system (1), with Assumptions 1 and 2, we denote

$$T = [T_1 \quad T_2], \quad S^{-1} = \left[S_{I,1}^\top\ S_{I,2}^\top\right]^\top, \tag{3}$$

where $T_1 \in \mathbb{R}^{n\times p_\star}$ and $S_{I,1} \in \mathbb{R}^{p_\star \times q}$. Thanks to the fact that C_{11} is invertible, the estimates of $\zeta_1(t)$ can be retrieved directly from the measurement

$$\hat{\zeta}_1(t) = C_{11}^{-1} S_{I,1} y(t). \tag{4}$$

Similarly, $\eta_2(t)$ can be obtained by transforming the output $\hat{\eta}_2(t) = S_{I,2}y(t)$. By recalling the fact that $\mathcal{S}_{\zeta_2}$ is detectable, a non-asymptotic state observer can be designed for system (2). For simplicity, in this paper we assume $\mathcal{S}_{\zeta_2}$ is a single-output system[1], *i.e.* $\eta_2(t) \in \mathbb{R}$ and $C_{22} \in \mathbb{R}^{1\times(n-p_\star)}$. A linear transformation P is introduced, so that $\mathcal{S}_{\zeta_2}$ can be rewritten in the observer canonical form with $z(t) = P\zeta_2(t)$:

$$\begin{cases} \dot{z}(t) &= A_c z(t) + A_{c,21}\zeta_1(t) + B_c u(t) \\ \eta_2(t) &= C_c z(t), \end{cases} \tag{5}$$

where $C_c = C_{22}P^{-1} = [1\ 0\ \dots\ 0]$,

$$A_c = PA_{22}P^{-1} = \begin{bmatrix} a_{n_\star-1} & 1 & 0 & \cdots & 0 \\ a_{n_\star-2} & 0 & 1 & \ddots & \vdots \\ \vdots & \vdots & \ddots & \ddots & 0 \\ a_1 & 0 & \dots & 0 & 1 \\ a_0 & 0 & \cdots & 0 & 0 \end{bmatrix},$$

where $n_\star = n - p_\star$ and $\{a_i, i \in \{0,1,\dots,n_\star - 1\}\}$ denotes the coefficients of the characteristic polynomial of the subsystems determined by the eigenvalues of matrix A_{22}. Moreover, $A_{c,21} = PA_{21}[\alpha_{n_\star-1}^\top, \alpha_{n_\star-2}^\top, \dots, \alpha_0^\top]^\top$ and

$$B_c = PB_2 = \begin{bmatrix} b_{0,n_\star-1} & b_{0,n_\star-2} & \dots & b_{0,0} \\ b_{1,n_\star-1} & b_{1,n_\star-2} & \dots & b_{1,0} \\ & & & \\ b_{m-1,n_\star-1} & b_{m-1,n_\star-2} & \dots & b_{m-1,0} \end{bmatrix}^\top.$$

Let us consider a type of Bivariate Feedthrough Non-asymptotic Kernel (BF-NK) proposed in [11] :

$$K_h(t,\tau) = e^{-\omega_h(t-\tau)}(1 - e^{-\bar{\omega}t})^N, \tag{6}$$

satisfying the condition $K_h^{(i)}(t,0) = 0$, $\forall i \in \{0,\dots,N-1\}$. We consider the set of BF-NKs parameterized with the same $\bar{\omega}$ but different ω_h, $h \in \{0 \dots n_\star - 1\}$. Moreover, we set $N \geq n_\star - 1$ so that the kernel is of at least $n_\star$-th order of non-asymptoticity. Applying the Volterra operator to the system $\mathcal{S}_{\zeta_2}$ and after some algebra, one can obtain

$$\nu(t) = \Gamma(t)z(t) \tag{7}$$

where $\nu(t) = [\mu_0(t), \mu_1(t), \dots, \mu_{n_\star-1}(t)]^\top$, $\Gamma(t) = \left[\gamma_0(t)^\top, \gamma_1(t)^\top, \dots, \gamma_{n_\star-1}(t)^\top\right]^\top$ and $\forall h \in \{0,\dots,n_\star-1\}$

$$\begin{aligned} \mu_h(t) &\triangleq (-1)^{n_\star-1}\left[V_{K^{(n_\star)}}\,\eta_2\right](t) + \sum_{i=0}^{n_\star-1} a_i(-1)^i\left[V_{K^{(i)}}\eta_2\right](t) \\ &+ \sum_{k=0}^{m-1}\sum_{i=0}^{n_\star-1}(-1)^i b_{k,i}\left[V_{K^{(i)}}u_k\right](t) + \sum_{i=0}^{n_\star-1}(-1)^i\alpha_i\left[V_{K^{(i)}}\zeta_1\right](t) \\ \gamma_h(t) &\triangleq \Big[(-1)^{n_\star-1}K^{(n_\star-1)}(t,t), \dots, K(t,t)\Big]. \end{aligned} \tag{8}$$

[1]A multi-output system can be reduced to single-output systems, for instance, using the output counterpart of input reduction technique [16].

For Volterra transformation calculation, the signal images are defined as $[V_{K_h^{(i)}}\star](t) \triangleq \xi_{\star,i,h}(t)$, where $\star(t)$ represents signals $\eta_2(t)$, $u_k(t)$ and $\zeta_1(t)$ respectively. The auxiliary signals $\xi_{\star,i,h}(t)$ can be calculated by

$$\xi^{(1)}_{\star,i,h}(t) = -\omega_h \xi_{\star,i,h} + K_h^{(i)}(t,t)\star(t), \tag{9}$$

with $\xi_{\star,i,h}(0) = 0$, $\forall h, i, \star(t)$.

Thanks to the specific shape of kernel defined in (6), the persistency of excitation of $\gamma_h(t)$ guarantees the invertibility of $\Gamma(t)$. Therefore, the state estimation of system (5) can be immediately obtained as

$$\hat{z}(t) = \Gamma(t)^{-1}\nu(t). \tag{10}$$

Consequently, the state variables in $\mathcal{S}_{\zeta_2}$ can be retrieved as $\hat{\zeta}_2(t) = P^{-1}\hat{z}(t)$ and, thanks to (4), the estimated state vector of the original system can be computed

$$\hat{x}(t) = T_1\hat{\zeta}_1(t) + T_2\hat{\zeta}_2(t). \tag{11}$$

B. Fault detection and isolation

Thanks to the fact that the state estimation enjoys a non-asymptotic convergence, the detection and isolation of the fault can be performed in a fast and accurate way. Recall the process $\mathcal{S}_{\zeta_1}$ in (2). If E_1^{-1} is invertible, the fault signal verifies the following identity

$$f = E_1^{-1}(\dot{\zeta}_1(t) - A_{11}\zeta_1(t) - A_{12}\zeta_2(t) - B_1u(t)), \tag{12}$$

where $\zeta_1(t)$ and $\zeta_2(t)$ can be estimated exactly while the derivative $\dot{\zeta}_1(t)$ becomes the main obstacle for detecting and identifying the fault signal promptly and accurately. Inspired by another kernel-based non-asymptotic estimation method detailed in [10], the lack of knowledge of the derivative can be addressed by the Volterra operator with a type of Bivariate Causal Non-asymptotic Kernel (BC-NK) which, for given $i \geq 1$, satisfies

$$F^{(j)}(t,0) = 0, F^{(j)}(t,t) = 0 \tag{13}$$

$\forall t \in \mathbb{R}_{\geq 0}$ and $\forall j \in \{0, ..., i-1\}$.

Applying the Volterra operator induced by a 1-st order BC-NK function

$$F(t,\tau) \triangleq e^{-\omega(t-\tau)}(1-e^{-\omega\tau})[1-e^{-\omega(t-\tau)}], \tag{14}$$

with the only tuning parameter ω, to (12), one can get

$$\begin{aligned}[V_F f](t) &= E_1^{-1}\big(-[V_{F^{(1)}}\zeta_1](t) - A_{11}[V_F\zeta_1](t) \\ &\quad -A_{12}[V_F\zeta_2](t)\big) - B_1[V_Fu](t)\big),\end{aligned} \tag{15}$$

in the light of the fact that

$$[V_F\zeta_1^{(i)}](t) = (-1)^i[V_{F^{(i)}}\zeta_1](t). \tag{16}$$

Remarkably, the kernel function (14) can be rearranged as

$$\begin{aligned}F(t,\tau) &= F_{0,1}(t,\tau) + F_{0,2}(t,\tau) \\ F^{(1)}(t,\tau) &= F_{1,1}(t,\tau) + F_{1,2}(t,\tau),\end{aligned} \tag{17}$$

where

$$\begin{aligned}F_{0,1}(\tau) &= (e^{\omega\tau}-1)e^{-\omega t} \\ F_{0,2}(\tau) &= (e^{\omega\tau}-e^{2\omega\tau})e^{-2\omega t} \\ F_{1,1}(\tau) &= \omega e^{\omega\tau}e^{-\omega t} \\ F_{1,2}(\tau) &= (\omega e^{\omega\tau} - 2\omega e^{2\omega\tau})e^{-2\omega t}.\end{aligned}$$

As a result, the image functions $\chi_{\star,i} = [V_{F^{(i)}}\star]$ of the signal can be calculated based on the state estimates by an internally stable LTV system

$$\begin{cases}\varsigma^{(1)}_{\star,i}(t) &= G\varsigma_{\star,i}(t) + E_i(t)\star(t) \\ \chi_{\star,i}(t) &= H\varsigma_{\star,i}(t),\end{cases} \tag{18}$$

where $i = \{0,1\}$ and $\star$ represents for $\zeta_1(t)$ and $\hat{\zeta}_2(t)$

$$\begin{aligned}G &= diag(-\omega, -2\omega) \\ E_i(t) &= [F_{i,1}(t,t), F_{i,2}(t,t)]^\top \\ H &= [1\ \ 1].\end{aligned}$$

In this way, it is possible to estimate in a non-asymptotic way the images of the fault function. We exploit this notable property for fault detection purposes. Hence, a fault detection residual

$$\begin{aligned}r_{FD}(t) &\triangleq \|[V_F f](t)\| \\ &= \|E_1^{-1}\big(-[V_{F^{(1)}}\zeta_1](t) - A_{11}[V_F\zeta_1](t) \\ &\quad -A_{12}[V_F\hat{\zeta}_2](t) - B_1[V_Fu](t)\big)\|,\end{aligned} \tag{19}$$

can be calculated to monitor the health status of the system, where $\|\cdot\|$ denotes the Euclidean norm.

Fault detection decision In noise-free conditions, a fault occurring in the system is detected by the proposed fault detection scheme at time $t = T_d$ if the fault detection residual $r_{FD}(t)$ is different from zero, i.e. $r_{FD}(T_d) \neq 0$.

After the detection of the fault, a fault isolation mechanism is activated by resetting the estimator (15), which means resetting all the transformations in (18). For the fault isolation purpose, a set of faults $\mathcal{F}$ is assumed to contain all the $N_\mathcal{F}$ possible fault functions $\phi_i(t,x,u)$, $i \in \{0,\ldots,N_\mathcal{F}-1\}$. In the noise-free scenario, the exact estimation of the state vector $\hat{x}(t)$ makes it possible to compute the effect of all the possible faults $\phi_i(t,\hat{x},u)$ in the fault set $\mathcal{F}$. Via the Volterra operator, the images of the possible fault functions $[\breve{V}_F\phi_i](t)$ are compared to the estimated fault image $[\breve{V}_F\phi](t)$ in (15), where for convenience, a new notation is deployed representing the operator after the resetting at $t = T_D$:

$$[\breve{V}_F\phi](t) \triangleq \int_0^{t-T_D} F(t-T_D,\tau)\phi(\tau+T_D)d\tau, \forall t \geq T_D. \tag{20}$$

Owing to the linearity of the Volterra operator, the satisfaction of the identity (15) can be preserved by this modified operator. Therefore, fault isolation residuals for every possible fault function in $\mathcal{F}$ are defined:

$$r_{FI,i}(t) \triangleq \|[\breve{V}_F\phi_i](t) - [\breve{V}_F\phi](t)\|, \forall i \in \{0,\ldots,N_\mathcal{F}-1\}. \tag{21}$$

Fault isolation In a noise-free scenario, by using the fault isolation residual (21), the p-th fault is excluded if $r_{FI,p}(t)$ is non-zero. If all the faults are excluded but the q-th one, i.e. $r_{FI,q} = 0$, $\forall t \geq T_D$, then q-th fault is isolated.

IV. Robustness Analysis

In this section we are going to analyze the performance of the estimation, fault detection and isolation algorithm in presence of additive disturbances on both the measurement and the process. We consider the following noise-perturbed model[2].

$$\begin{cases} \dot{x}_d(t) &= Ax_d(t) + Bu(t) + Ef(t,x,u) + d_x(t,x,u) \\ y_d(t) &= Cx_d(t) + d_y(t) \end{cases} \tag{22}$$

where we assume both the disturbances are bounded at each time step by two constants, *i.e.*

$$\|d_x(t,x,u)\| \leq \bar{d}_x, \ \|d_y(t)\| \leq \bar{d}_y.$$

The effect of the measurement noise directly appears on $\eta_1(t)$ and $\eta_2(t)$. With $\left[\eta_{d,1}^\top(t) \ \eta_{d,2}^\top(t)\right]^\top = S^{-1}y_d(t)$. This results in the error on the reconstruction of $\zeta_{1,d}(t)$:

$$|\epsilon_{\zeta_1}(t)| \triangleq |\hat{\zeta}_1(t) - \zeta_{1,d}(t)| \leq \|C_{11}\|\|S_{I,1}\|\bar{d}_y \triangleq \bar{\epsilon}_{\zeta_1}.$$

We define the following error vector:

$$|\epsilon_{\eta_2}(t)| = |\hat{\eta}_2(t) - \eta_{2,d}(t)| \leq \|S_{I,2}\|\bar{d}_y \triangleq \bar{\epsilon}_{\eta_2}. \tag{23}$$

Considering the perturbed subsystem $\mathcal{S}_{\zeta_2,d}$,

$$\dot{\zeta}_{2,d}(t) = A_{21}\zeta_{1,d}(t) + A_{22}\zeta_{2,d}(t) + B_2u(t) + d_{x,2}(t,x,u) \tag{24}$$

with $T^{-1}d_x = [d_{x,1}^\top(t) \ d_{x,2}^\top(t)]$ and $d_{x,2}(t) = [d_{x,2,n_\star-1}(t), \ldots, d_{x,2,0}(t)]^\top \in \mathbb{R}^{n_\star}$. Thus, in the noisy case, we obtain

$$\begin{aligned} \epsilon_{\zeta_2}(t) &\triangleq |\hat{\zeta}_2(t) - \zeta_{2,d}(t)| \\ &= \left|P^{-1}\Gamma(t)^{-1}\left[\epsilon_{\mu_0}(t), \epsilon_{\mu_1}(t), \ldots, \epsilon_{\mu_{n_{\xi}-1}}(t)\right]^\top\right| \end{aligned} \tag{25}$$

with

$$\begin{aligned} &\epsilon_{\mu_h}(t) \triangleq |\hat{\mu}_h(t) - \mu_h(t)| \\ &= (-1)^{(n_\star)}[V_{K^{(n_\star)}}\epsilon_{\eta_2}](t) - \sum_{i=0}^{n_\star-1} a_i(-1)^i[V_{K^{(i)}}\epsilon_{\eta_2}](t) \\ &-\sum_{i=0}^{n_\star-1}(-1)^i\alpha_i[V_{K^{(i)}}\epsilon_{\zeta_1}](t) - \sum_{i=0}^{n_\star-1}(-1)^i[V_{K^{(i)}}d_{x,2,n_\star-1-i}](t). \end{aligned}$$

Moreover, we notice that the BF-NK can be reshaped as

$$K(t,\tau) = e^{-\omega_h t}\sum_{q=0}^{n_\star}\binom{n_\star}{q}(\omega_h - q\bar{\omega})^i e^{(\omega_h - q\bar{\omega})\tau}. \tag{26}$$

Therefore, the BF-NK Volterra images of the signals admit upper bounds

$$[V_{K_h^{(i)}}\star](t) \leq \bar{\star}\int_0^t |K(t,\tau)|d\tau \leq \bar{\star}w_h^{i-1} \triangleq \bar{\xi}_{\star,i,h}, \tag{27}$$

[2]Variables with the subscript d denotes the noisy counterparts of the variables in (1).

where $\star(t)$ and $\bar{\star}$ represents the signals $\epsilon_{\zeta_1}(t)$, $\epsilon_{\zeta_2}(t)$, $d_{x,2}(t)$ and their corresponding upper bounds. Remarkably, ω_h can be properly tuned to reduce the bound, thus obtaining a tighter bound.

Remark 4.1: The computation of the estimation error bound (25) at the beginning of the simulation could have numerical issues as $\Gamma(t)$ is nearly singular close to the initial time instant, and therefore $\|\Gamma(t)^{-1}\|$ may have very large values at the beginning. Therefore, we deploy a threshold θ_a to activate the fault detection mechanism after a short period at $t = T_a$ when $det(\Gamma(t)) \geq \theta_a$. T_a is adjustable by tuning $\bar{\omega}$ in terms of the converging speed of the kernels.

Therefore, the afore-defined error (25) admits the bound

$$\epsilon_{\zeta_2}(t) \leq \|P^{-1}\Gamma(t_a)^{-1}\|\left\|\left[\bar{\epsilon}_{\mu_0}, \bar{\epsilon}_{\mu_1}, \ldots, \bar{\epsilon}_{\mu_{n_{\xi}-1}}\right]^\top\right\| \triangleq \bar{\epsilon}_{\zeta_2}, \tag{28}$$

$\forall t \geq T_a$, where

$$\begin{aligned} \bar{\epsilon}_{\mu_h} &= \bar{\xi}_{\epsilon_{\eta_2},n_\star,h} + \sum_{i=0}^{n_\star-1}|a_i|\bar{\xi}_{\epsilon_{\eta_2},i,h} \\ &+ \sum_{i=0}^{n_\star-1}|\alpha_i|\bar{\xi}_{\epsilon_{\eta_1},i,h} + \sum_{i=0}^{n_\star-1}\|T^{-1}\|\bar{\xi}_{\bar{d}_x,i,h}. \end{aligned}$$

Consequently, the estimation error of the state is bounded by

$$\begin{aligned} \|\epsilon_x\| &\triangleq \|\hat{x}(t) - x_d(t)\| \\ &\leq \|T_1\|\|\bar{\epsilon}_{\zeta_1}\| + \|T_2\|\|\bar{\epsilon}_{\zeta_2}\| \triangleq \bar{\epsilon}_x. \end{aligned} \tag{29}$$

By recalling (15), we can then define the error on the estimation of the fault image

$$\begin{aligned} \epsilon_{\chi_{f,0}}(t) = |\hat{\chi}_{f,0}(t) - \chi_{f,0}(t)| = \Big|E_1^{-1}\Big[-[V_{F^{(1)}}\epsilon_{\zeta_1}](t) \\ -A_{11}[V_F\epsilon_{\zeta_1}](t) - A_{12}[V_F\epsilon_{\zeta_2}](t) - [V_Fd_{x,1}](t)\Big]\Big|. \end{aligned} \tag{30}$$

Considering the Volterra images induced by BC-NK,

$$\begin{aligned} &[V_F \star](t) \leq \bar{\star}\left(\frac{1 - e^{-2\omega t}}{2\omega} - te^{-\omega t}\right) \triangleq \bar{\chi}_{\star,0}(t), \\ &[V_{F^{(1)}}\star](t) \leq \bar{\star}\int_0^t |F^{(1)}(t,\tau)|d\tau = \bar{\star}\frac{(e^{-\omega t} - 1)^2}{2} \triangleq \bar{\chi}_{\star,1}(t). \end{aligned} \tag{31}$$

Then, the estimation error of the fault image $\epsilon_{\chi_{f,0}}$ satisfies

$$\begin{aligned} &\|\epsilon_{\chi_{f,0}}(t)\| \ \leq \ \|E_1^{-1}\|\|\bar{\chi}_{\epsilon_{\zeta_1},1}(t)\| + \|E_1^{-1}A_{11}\|\|\bar{\chi}_{\epsilon_{\zeta_1},0}(t)\| \\ &+\|E_1^{-1}A_{12}\|\|\bar{\chi}_{\epsilon_{\zeta_2},0}(t)\| + \|E_1^{-1}\|\|T^{-1}\|\|\bar{\chi}_{d_x,0}(t)\| \triangleq \sigma_{FD}(t), \end{aligned} \tag{32}$$

which can be used as a threshold for fault detection σ_{FD} in the noisy scenario.

Proposition 4.1: A fault occurring in the system is detected by the proposed fault detection scheme at time $t = T_D$ once the fault detection residual $r_{FD}(t)$ exceeds the fault detection threshold $\sigma_{FD}(t)$, i.e. $r_{FD}(T_D) > \sigma_{FD}(T_D)$.

For what concerns the fault isolation problem in the noisy scenario, we can show that the images computed based on

the noisy measurements are bounded by

$$\begin{aligned}[\breve{V}_F \star](t) &\leq \bar{\chi}_{\star,0}(t-T_D) \triangleq \bar{\bar{\chi}}_{\star,0}(t)\\ [\breve{V}_{F^{(1)}} \star](t) &\leq \bar{\chi}_{\star,1}(t-T_D) \triangleq \bar{\bar{\chi}}_{\star,1}(t).\end{aligned} \tag{33}$$

Moreover, let us note the fact that the upper bounds of Volterra images defined in (27) and (33) is either constant or will increasingly converge to certain computable constant values. Therefore, it is reasonable to assume the reconstruction error of the fault functions in $\mathcal{F}$, introduced by the state estimation error, to have computable upper bounds

$$\bar{\epsilon}_{\phi_{r,i}} \triangleq \sup_{\forall t>T_a} \|\hat{\phi}_i(\tau,\hat{x},u) - \phi_i(\tau,x_d,u)\|, \tag{34}$$

for all $i \in \{0,\dots,N_{\mathcal{F}}-1\}$.

Therefore, the fault isolation residual for the i-th fault

$$\begin{aligned}r_{FI,i} &= \|[\breve{V}_F\hat{\phi}_i](t) - [\breve{V}_F\hat{\phi}](t)\|\\ &\leq \|[\breve{V}_F\hat{\phi}_i](t) - [\breve{V}_F\phi](t)\| + \|[\breve{V}_F\phi](t) - [\breve{V}_F\hat{\phi}](t)\|.\end{aligned} \tag{35}$$

Recall the fact that

$$\begin{aligned}[\breve{V}_F\hat{\phi}](t) = \Big|E_1^{-1}\Big(&- [\breve{V}_{F^{(1)}}\hat{\zeta}_1](t) - A_{11}[\breve{V}_F\hat{\zeta}_1](t)\\ &- A_{12}[\breve{V}_F\hat{\zeta}_2](t) - B_1[\breve{V}_F u](t)\Big)\Big|\\ [\breve{V}_F\phi](t) = \Big|E_1^{-1}\Big(&- [\breve{V}_{F^{(1)}}\zeta_{d,1}](t) - A_{11}[\breve{V}_F\zeta_{d,1}](t)\\ &- A_{12}[\breve{V}_F\zeta_{d,2}](t) - B_1[\breve{V}_F u](t) - [\breve{V}_F d_{x,1}]\Big)\Big|\end{aligned}$$

which turns out that

$$\begin{aligned}\|[\breve{V}_F\phi](t) - [\breve{V}_F\hat{\phi}](t)\| = \Big|E_1^{-1}\Big(&- [\breve{V}_{F^{(1)}}\epsilon_{\zeta_1}](t)\\ &- A_{11}[\breve{V}_F\epsilon_{\zeta_1}](t) - A_{12}[\breve{V}_F\epsilon_{\zeta_2}](t) - [\breve{V}_F d_{x,1}]\Big)\Big|.\end{aligned} \tag{36}$$

Therefore, by substituting (36) and (34) into (35), the fault isolation residual for the i-th fault in $\mathcal{F}$ can be bounded by

$$\begin{aligned}r_{FI,i}(t) \leq &\|\bar{\bar{\chi}}_{\bar{\epsilon}_{\phi_i}}(t)\| + \|E_1^{-1}\|\|\bar{\bar{\chi}}_{\epsilon_{\zeta_1},1}(t)\| + \|E_1^{-1}A_{11}\|\|\bar{\bar{\chi}}_{\epsilon_{\zeta_1},0}(t)\|\\ &+ \|E_1^{-1}A_{12}\|\|\bar{\bar{\chi}}_{\epsilon_{\zeta_2},0}(t)\| + \|E_1^{-1}\|\|T^{-1}\|\|\bar{\bar{\chi}}_{\bar{d}_x,0}(t)\| \triangleq \sigma_{FI}(t),\end{aligned} \tag{37}$$

thus obtaining the corresponding fault isolation thresholds, for all $i \in \{0,\dots,N_{\mathcal{F}}-1\}$.

Proposition 4.2: By using the fault isolation residual (35) and the fault isolation threshold, the p-th fault is excluded at $T_{E,p}$ if $r_{FI,p}(t)$ exceeds the corresponding threshold *i.e.* $\exists\, T_{E,p} \geq T_D$ such that $r_{FI,i}(T_{E,p}) > \sigma_{FI,p}(T_{E,p})$. If all the faults are excluded but one, i.e. $r_{FI,q} \leq \sigma_{FI,q}(t)$, at $t = T_I \geq T_D$, then the q-th fault is isolated.

V. Numerical Example

In this section, we consider the following linear system as in [17]

$$\begin{cases}\dot{x}(t) &= Ax(t) + Bu(t) + Ef(t,x,u)\\ y(t) &= Cx(t)\end{cases} \tag{38}$$

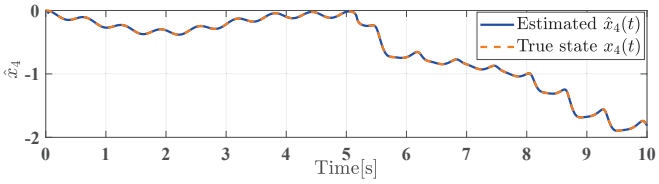

Fig. 1. Estimation of state variable $x_4(t)$ in noise-free scenario.

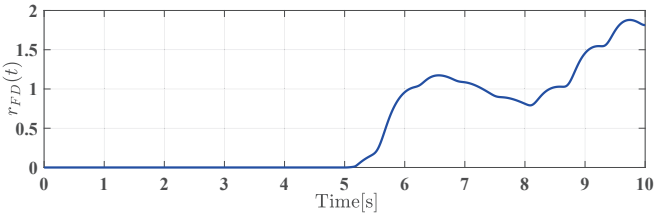

Fig. 2. Fault detection residual $r_{FD}(t)$ in noise-free scenario.

with

$$A = \begin{bmatrix} -0.6344 & 0.0022 & -0.0001 & 0.9871 & 0.0010\\ 0 & -0.2912 & 0.1026 & 0 & -0.3707\\ 0 & -6.2354 & -0.4312 & 0 & -4.1270\\ -0.5971 & 0.0003 & 0.0001 & -0.5099 & 0.0006\\ 0 & -0.4528 & -0.0481 & 0 & -0.9513 \end{bmatrix},$$

$$B = \begin{bmatrix} -0.0459\\ -0.0047\\ 3.7830\\ -2.5115\\ -0.0453 \end{bmatrix}, \quad C = \begin{bmatrix} 1 & 0 & 0 & 0 & 0\\ 0 & 1 & 0 & 0 & 0\\ 0 & 0 & 1 & 0 & 0\\ 0 & 0 & 0 & 1 & 0 \end{bmatrix},$$

$$E = \begin{bmatrix} -0.0395 & -0.0133 & -1.0000\\ 0 & 0.0031 & 0\\ 0 & 1.8255 & -0.5000\\ -1.9042 & -0.9494 & -1.0000\\ 0 & -0.2081 & 0 \end{bmatrix},$$

and $x(0) = [x_0(0),\dots,x_4(0)] = \mathbf{0}_{5\times 1}$. The system is fed by the signal $u(t) = 10\sin(10t) + \sin(2t)$. We assume two possible faults in the fault set, *i.e.*

$$\begin{aligned}\mathcal{F} = \Big\{&\phi_1(t) = [x_1(t) + x_2(t),\, \cos(x_3(t)),\, \cos(0.5x_4(t))]^\top,\\ &\phi_2(t) = [x_1(t) + x_2(t),\, 20e^{(-|x_3(t)|)},\, \sin(0.5x_4(t))]^\top\Big\},\end{aligned}$$

and $\phi_2(t)$ is the fault actually occurring at $t = 5s$, *i.e.* $f(t) = \mathcal{B}(t-5)\phi_2(t)$. For this system, it is readily seen that $p_\star = 3$ and $n_\star = 2$. By choosing the proper order of the kernel, with $\omega_1 = 1$, $\omega_2 = 2$, $\omega_3 = 3$, $\bar{\omega} = 2.5$ and $\omega = 1$, the performance of the proposed estimation and FDI scheme in the noise-free scenario are depicted in Fig. 1-3.

Estimates of the x_4 (the fifth and the only state variable that does not appears in the output) is shown as an example of state estimation in Fig. 1, instantaneous convergence can be seen in the estimation of the state variable, non-sensitive to the occurrence of the fault. Moreover, the fault detection residual increases immediately after the occurrence of the fault, thus achieving fast fault detection. The fault detection

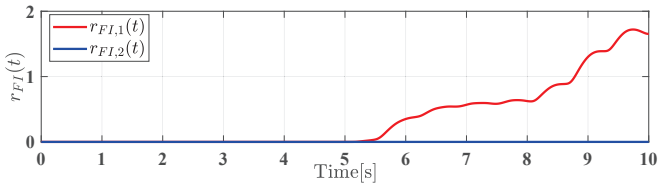

Fig. 3. Fault isolation residual $r_{FI,i}(t)$ in noise-free scenario.

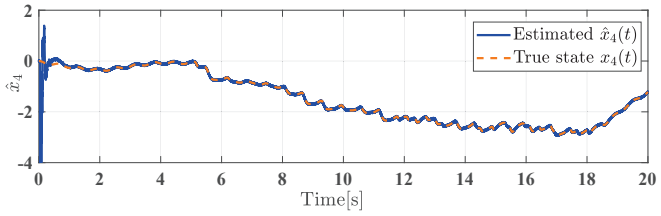

Fig. 4. Estimation of state variable $x_4(t)$ in noisy scenario.

decision activates the fault isolation estimator. Consequently, the residual of $\phi_1(t,x,u)$ increases and $\phi_2(t,x,u)$ remains at 0, indicating that it is $\phi_2(t,x,u)$ affecting the system.

Then, we examine the estimator performance in a scenario where the measurement $y(t)$ is corrupted by a random additive noise $d_y(t)$ ranging within $[-0.5, 0.5]$ and the system is perturbed with a process noise $d_x(t)$ ranging randomly within $[-0.2, 0.2]$. We set the activation threshold $\theta_a = 0.7$.

When the system is perturbed by both the measurement and the process noises, the proposed estimator is still able to provide fast estimates of the state variables albeit with bounded estimation error (see Fig. 4). Meanwhile, with the threshold $\sigma_{FD}(t)$ in (32), the occurrence of the fault can be detected at $T_d = 6.168s$. In the fault isolation scheme, the residual $r_{FI,1}(t)$ keeps increasing and crosses the threshold $\sigma_{FI,1}(t)$ at $T_i = 11.755s$ while $r_{FI,2}(t)$ remains lower than $\sigma_{FI,2}(t)$, thus isolating the occurrence of $\phi_2(t,x,u)$ and excluding $\phi_1(t,x,u)$.

VI. Concluding Remarks

In this paper, a fast fault detection and isolation scheme is proposed based on Volterra integral operators. The estimation of the state converges immediately to the true system state insensitive to the occurrence of the fault in the ideal noise-free case. Furthermore, based on the deadbeat estimation of the Volterra image of the fault signal, the occurrence time and the type of the fault can be identified immediately once the fault occurs. In the noisy scenario, thresholds are calculated based on the bound of the estimation error, to achieve robust fault detection and isolation. Future research efforts will be devoted to the fault detectability analysis and the extension to a distributed FDI architectures.

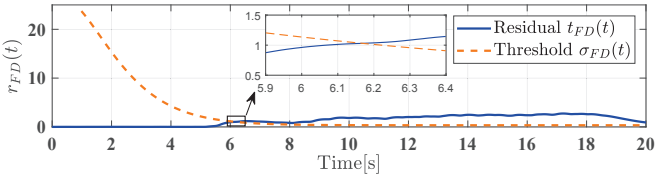

Fig. 5. Fault detection residual $r_{FD}(t)$ in noisy scenario.

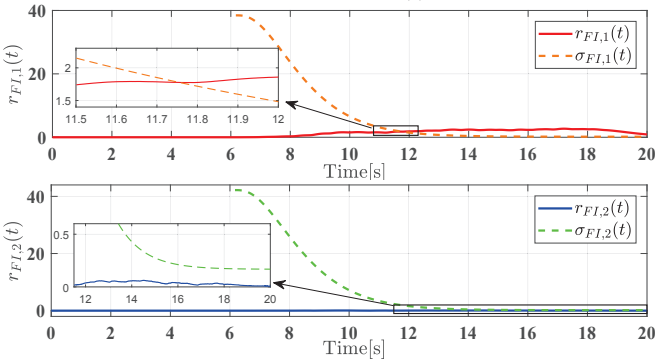

Fig. 6. Fault isolation residual $r_{FI,i}(t)$ in noisy scenario.

References

[1] R. J. Patton, P. M. Frank, and R. N. Clarke, Eds., *Fault Diagnosis in Dynamic Systems: Theory and Application*. Prentice-Hall, Inc., 1989.

[2] M. Blanke, M. Kinnaert, J. Lunze, M. Staroswiecki, and J. Schröder, *Diagnosis and fault-tolerant control*. Springer, 2006, vol. 2.

[3] J. Gertler, *Fault Detection and Diagnosis*. Springer, 2015.

[4] S. Simani, C. Fantuzzi, and R. J. Patton, *Model-based fault diagnosis in dynamic systems using identification techniques*. Springer Science & Business Media, 2013.

[5] V. Reppa, M. M. Polycarpou, and C. G. Panayiotou, "Decentralized isolation of multiple sensor faults in large-scale interconnected nonlinear systems," *IEEE Transactions on Automatic Control*, vol. 60, no. 6, pp. 1582–1596, 2015.

[6] J. Lan and R. J. Patton, "A new strategy for integration of fault estimation within fault-tolerant control," *Automatica*, vol. 69, pp. 48–59, 2016.

[7] M. Blanke, M. Kinnaert, J. Lunze, and M. Staroswiecki, "Distributed fault diagnosis and fault-tolerant control," in *Diagnosis and Fault-Tolerant Control*. Springer, 2016, pp. 467–518.

[8] M. R. Davoodi, K. Khorasani, H. A. Talebi, and H. R. Momeni, "Distributed fault detection and isolation filter design for a network of heterogeneous multiagent systems," *IEEE Transactions on Control Systems Technology*, vol. 22, no. 3, pp. 1061–1069, 2014.

[9] F. Boem, R. M. Ferrari, C. Keliris, T. Parisini, and M. M. Polycarpou, "A distributed networked approach for fault detection of large-scale systems," *IEEE Transactions on Automatic Control*, vol. 62, no. 1, pp. 18–33, 2017.

[10] G. Pin, A. Assalone, M. Lovera, and T. Parisini, "Non-asymptotic kernel-based parametric estimation of continuous-time linear systems," *IEEE Transaction on Automatic Control*, vol. 61, no. 2, pp. 360–373, 2016.

[11] G. Pin, M. Lovera, A. Assalone, and T. Parisini, "Kernel-based non-asymptotic state estimation for linear continuous-time system," in *2013 IEEE American Control Conference*, Washington, DC, 2013, pp. 3123–3128.

[12] P. Li, F. Boem, G. Pin, and T. Parisini, "Deadbeat simultaneous parameter-state estimation for linear continuous-time systems: a kernel-based approach," to appear in European Control Conference (ECC). IEEE, 2018.

[13] ——, "Distributed fault detection and isolation for interconnected systems: a non-asymptotic kernel-based approach," *IFAC-PapersOnLine*, vol. 50, no. 1, pp. 1013–1018, 2017.

[14] M. Corless and J. Tu, "State and input estimation for a class of uncertain systems," *Automatica*, vol. 34, no. 6, pp. 757 – 764, 1998. [Online]. Available: http://www.sciencedirect.com/science/article/pii/S0005109898000132

[15] T. A. Burton, *Volterra integral and differential equations*. Elsevier, 2005, vol. 202.

[16] J. C. Willems and J. W. Polderman, *Introduction to mathematical systems theory: a behavioral approach*. Springer Science & Business Media, 2013, vol. 26.

[17] W. Chen and M. Saif, "Fault detection and isolation based on novel unknown input observer design," in *American Control Conference, 2006*. IEEE, 2006, pp. 6–pp.